ISSN:2372-0743 print
ISSN:2373-2989 on line
International Journal of Ground Sediment & Water
Vol. 18
2023

◆Research Paper

DOI: 10.5281/zenodo.7861995

Engineering Geological Highway Structural Failure Assessment and Modeling of its Geotechnical Parameters: Case Study of Failed F- 209 Pavement, Southwestern Nigeria

Olumuyiwa Olusola Falowo[1,2*], Tosin Anthony Oniyelu[2]

1Department of Geology, Federal University of Technology Akure, Ondo State, Nigeria

[2]Department of Civil Engineering Technology, Rufus Giwa Polytechnic, Owo, Ondo State, Nigeria

Email id: oluwanifemi.adeboye@yahoo.com

ORCID: http://orcid.org/0000-0003-3425-9072

Abstract: Engineering geological investigation of the soil domain along the highway alignment of F-209 connecting Akure and Ado-Ekiti Southwestern Nigeria, had been investigated to assess the structural failure of the highway. Findings showed that the subsoil delineated is characterized by resistivity ranging from 135 – 711 ohm-m (avg. 385 ohm-m) composing sandy clay and clay sand (predominant). The soils are of intermediate plasticity/compressibility; and montmorillonite clay mineralogy group. The soaked CBR/in-situ CBR values are generally less than 10% minimum specification for subgrade materials. The GI values (avg. 13) corresponded to poor subgrade soil. Based on the GI and CBR values, the recommended thickness of the pavement should range from 267 mm (good segment) to 521 mm (for the weak segment) (avg. 401 mm, but are far above the present thickness of 159 – 210 mm. Therefore the present design thickness of the highway can't sustain the vehicular loads/haulage activities on the highway. The SNG contribution of the soil as subgrade material (avg. 0.48), strength coefficient of the soil as subbase (avg. 0.0671) and base (avg. 0.0357) in terms of SN/SNC and SNP are less than 0.5 minimum required for pavement strength/layer contribution. Parameter modelling showed all showed strong positive correlations except soaked CBR Vs in-situ and RD Vs DCPI that displayed weak

positive correlations. The validity of the models is based on applicability and accuracy. Therefore, the highway failure can be attributed to weak geologic and engineering properties, coupled with inadequate design thickness and lack of drainage facility at the shoulders.

Keywords: CBR, penetrative index, elastic modulus, geotechnical, structural number, subgrade modulus.

Introduction

Road transportation is an important indicator of economic and social progress since it facilitates access to inaccessible areas (Wright, 1997; Adetoro and Abe, 2018; Ifarajimi et al., 2021). Over the years, the Nigerian government has made significant investments in road infrastructure development and upkeep, including repair, rehabilitation, and/or upgrading of existing pavement. However, many Nigerian roads are rapidly deteriorating due to a variety of factors such as poor design and construction, heavy traffic, poor maintenance culture, poor highway facilities, use of low-quality materials, poor workmanship, poor supervision, low knowledge base, compromising local standards of practice, usage, ageing (Okigbo, 2012; Owoseni, 2019; Osuolale et al., 2012), and so on; and these failures are manifested in the form of potholes, rutting, corrugation, ravelling, flushing, cracks (alligator, traverse and longitudinal cracks). Many of these road failures are the consequence of functional and structural issues, which are increasing government recurrent expenditures year after year. Occasionally, a highway reconstruction or rehabilitation project is granted to a contractor with no commensurate influence on the project; and where they carry out the project, it was discovered that they discard many of the preparatory studies engaged in site assessment or soil exploration.

The route between Akure and Ado Ekiti is one of the busiest in Southwestern Nigeria, connecting the northern and southern parts of the country (Fig. 1). It is a section of the F-209 Federal Government Road, having a total length of 45 meters (45 m). The road had collapsed over five years before. Although the Ekiti State government, in collaboration with the Federal government, repaired the failed segment between Ado and Ikere Ekiti some years ago, it recently failed again, without meeting the designed life expectancy; and there is

no appropriate sanction from the government for such substandard jobs. When travelling to Ekiti State and the northern part of the nation, commuters prefer choosing the Igbara - Odo - Ilawe route rather than the Akure - Ado route (Fig. 1). The current status of the road has hampered the social and economic growth of the area it traverses. Many roads, both new and old, have failed owing to inadequate laboratory and in-situ examinations of the soil within the road alignment. As a result, it became critical to make essential geotechnical and geophysical parameters of the subsoil beneath the highway available in preparation for highway reconstruction (even though the reconstruction/rehabilitation had commenced from the Ado - Ikere axis), as illustrated in Fig. 2. Clearly, the objectives of this study are to identify and classify the subsoil within the road alignment; assess the subsoil geological, geochemical, and geotechnical properties concerning soil domain competence based on destructive and non-destructive in-situ tests/survey and laboratory studies; determine important geotechnical correlations and parameters modelling for the highway; and investigate any geological structure that may be detrimental to the stability of the highway.

Site Description and Geology

The F-209 Akure – Ado Ekiti Highway links Ondo with Ekiti States, both in Southwestern Nigeria. It has undulating topography as some zones of the pavement were cut through geological formations, and these zones are windy.

The highway is about 45 km, but only 38 km of road length was investigated in this study. The study started from Ado Garage in Akure with geographical coordinates in Universal Traverse Mercator (UTM) of 0747073 mE and 0809685 mN and terminated in Ado after Oluwasola Block Industry with coordinates of 746062mE and 0839316mN. The area is characterized by wet and dry seasons. The rainy season lasts from April to October, while the dry season lasts from November to February. The annual rainfall and temperature average 1500 mm and 24 °C, respectively (Iloeje, 1981). June and September are typically wet months with relative humidity around 80%, though this can drop to less than 50% during the dry season (Federal Meteorological Survey, 1982). The highway is situated within Basement Complex of Southwestern Nigeria (Fig. 2). The road alignment cuts across three geologic units comprising the migmatite, granite, and charnockite. The southern segment is

predominantly migmatite and granite, while at Ita-ogbolu to Ikere is charnockite/granite; and Ado Ekiti segment is granite (Figs 3-4).

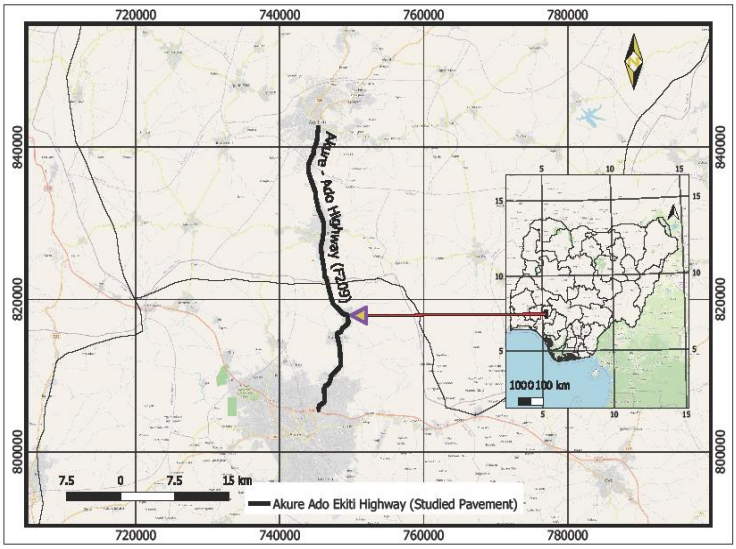

Fig. 1 Map of the Studied Highway. Inset: Map of Nigeria showing the location of the Akure – Ado Highway in southwestern Nigeria

Material and Methods

Dynamic Cone Penetration Test (DCPT)

An integrated Dynamic cone penetration test, geophysics using VES; laboratory geotechnical and geochemical analysis; trial pit excavation (depth of 1.0 m); and groundwater level measurement were used in this investigation to determine the presence of any spring or artesian well along the route. Fig. 5 depicts the study's data acquisition map. The DCPT was taken along the roadway at around 1.0 to 5.0 m offset from the highway's edge, using ASTM-D 6951-3 (2003) procedure. The DCP is a simple mechanical device that can provide 45.5 Joules of energy and is used for quick in-situ strength assessment of roadway structural material, particularly the subgrade and other unbound layers (Ilori, 2015; Anon, 1952; Chen et al., 2005; De Beer and van der Merwe, 1991).

It measures the penetration of a standard cone when a standard force is applied (Done and Samuel, 2006; Hassan, 1996). The DCP penetrative index in mm per standard hammer blow is recorded, together with the number of blows and depth of penetration. The

conventional steel cone with an angle of 60° and a diameter of 20 mm was employed in this investigation (Paige-green and Zyl, 2019).

The standard 8 kg hammer, which glides along a 16 mm diameter steel rod with a fall height of 575 mm and impacts the anvil to produce penetration, was also used (Done and Samuel, 2006; Putra et al., 2021). The test was carried out at ten (10) different points along the roadway (Fig. 6). This low test number was attributed to the insecurity that was typical of failing roadways. The data gathered was analyzed and interpreted using the UK DCP 3.1 program. The data acquired at each location was adjusted for moisture content before being used to calculate the CBR using the Transport and Road Research Laboratory - TRL (1990) relationship as shown in Table 1. From Test No. 1 to Test No. 10, each test site was serially numbered. The hammer factor, also known as the coefficient, is 1.0.

Fig. 2 Pictures showing the investigated Highway during the reconstruction/rehabilitation

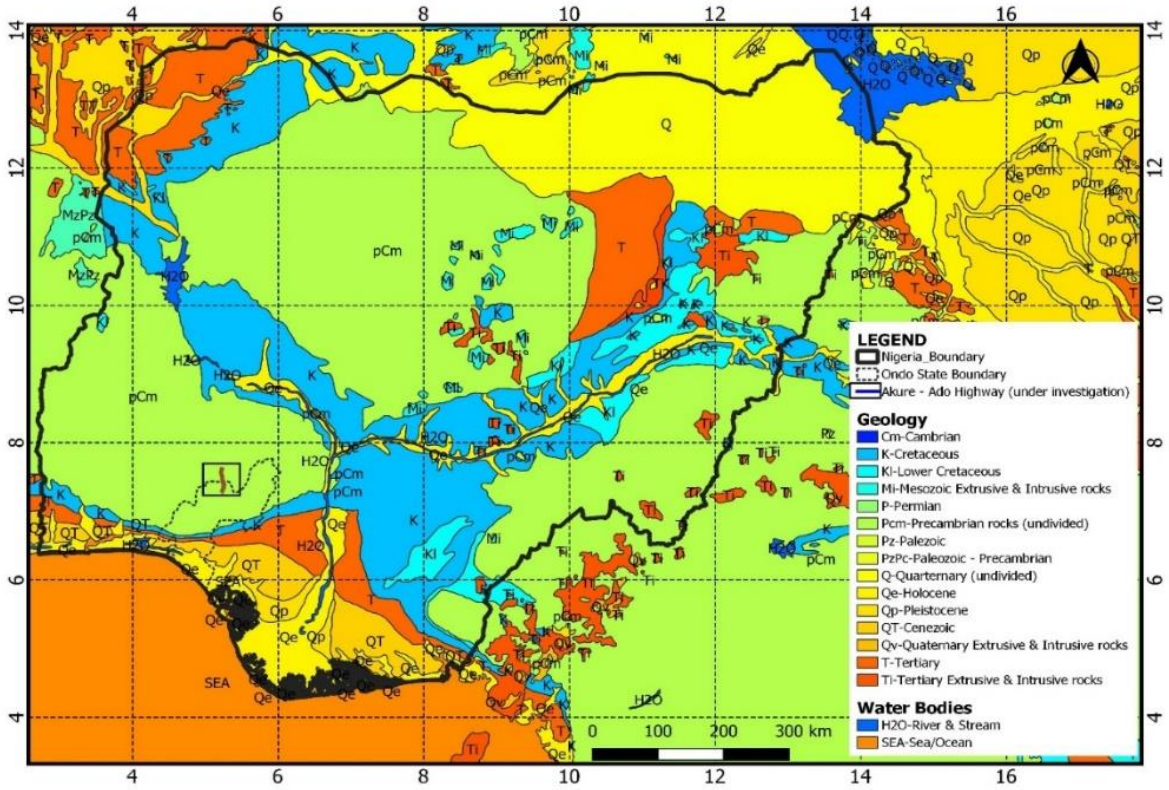

Fig. 3 Geological map of Nigeria showing the highway under investigation (modified after Nigerian Geological Survey Agency, 2006)

The UK DCP 3.1 determined the strength coefficient of the test sites by converting the penetration rate to CBR value, then to strength coefficient, and lastly to structural number. As indicated in Equation 1, the TRL equation was utilized to calculate CBR. The subsoil strength coefficient for use as the base and subbase layers are derived using equations 2 (for base) and 3 (for subbase).

$$\mathrm{Log}_{10}^{(\mathrm{CBR})} = 2.48 - 1.057\ \mathrm{Log}_{10}^{(\text{pen rate})} \tag{1}$$

$$\mathrm{a} = 0.0001[29.14\ (\mathrm{CBR}) - 0.1977\ (\mathrm{CBR})^2 + 0.00045\ (\mathrm{CBR})^3 \tag{2}$$

$$\mathrm{a} = 0.184\ \mathrm{Log}_{10}^{(\mathrm{CBR})} - 0.0444\ \left(\mathrm{Log}_{10}^{(\mathrm{CBR})^2}\right) - 0.075 \tag{3}$$

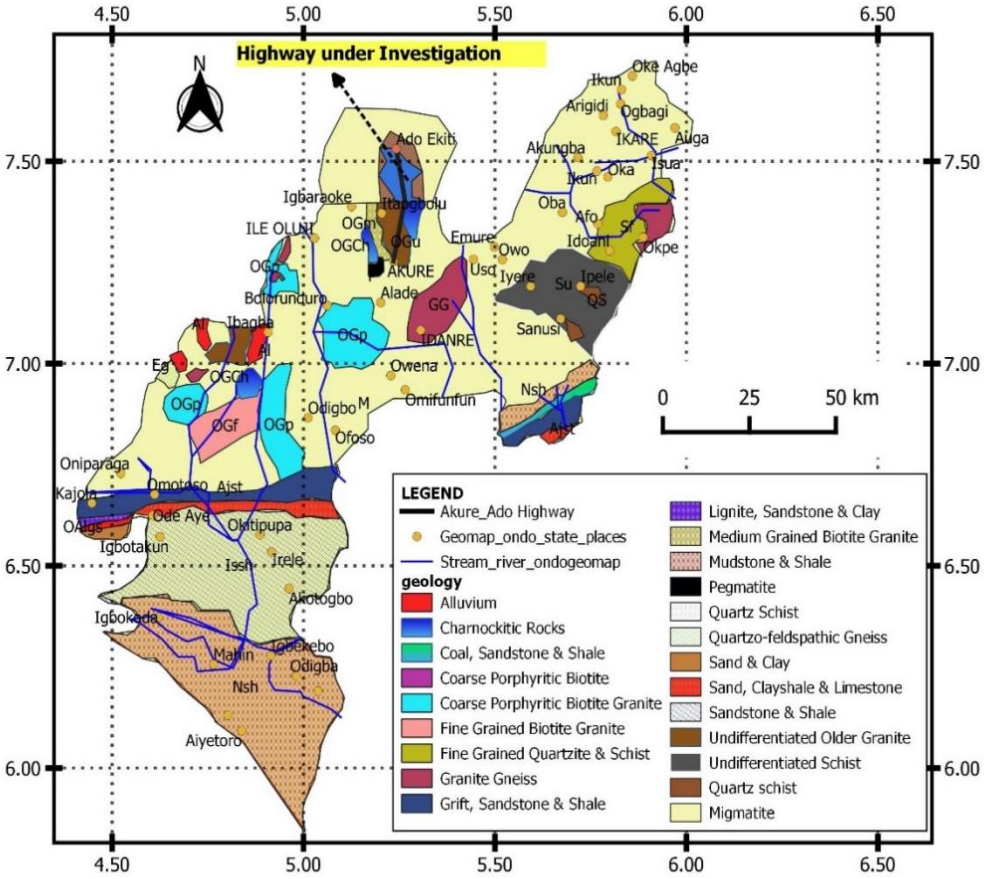

Fig. 4 Geological Map of Ondo State and Part of Ekiti showing the road under investigation straddling migmatite, older granite and charnockitic rocks (modified after NGSA, 1984).

The SNG, also known as the subgrade structural number, is the contribution of subgrade material to the structural number of a pavement. It is often generated from CBR, as well as the base and base layers (Done and Samuel, 2006). Equation 4 shows the relationship between SNG and CBR.

$$\mathrm{SNG} = 3.51\,\mathrm{Log}_{10}^{(\mathrm{CBR})} - 0.85\,\mathrm{Log}_{10}^{(\mathrm{CBR})^2} - 1.43 \qquad (4)$$

The relative densities of each subsoil stratum were calculated using the DIN 4094 (DIN 4094 Part 2, 180) model (equation 5, where n10 is the number of blows for every 10 cm). The resilient modulus (using Lockwood et al., 1992; George and Uddin, 2000; and Jianzhou et al., 1999 models, as shown in equations 6 – 8 respectively) and Young modulus were obtained from each site along the highway alignment using Equation 9. From the results,

important correlations and parameters modelling were obtained between M_R and E_R, M_R and CBR, DCPI and relative density, and CBR and relative density.

$$I_D = 0.21 + 0.230 \log n_{10} \quad (5)$$

$$M_R = 10^{3.04758 - 1.06166 \log[DCPI)} \quad (6)$$

$$M_R = 235.3 \times DCPI^{-0.475} \quad (7)$$

$$\mathrm{M_R} = 338 \times \mathrm{DCPI}^{-0.39} \quad (8)$$

$$\mathrm{E_R} = \frac{\mathrm{M_R} - 12.69}{1.065} \quad (9)$$

Geophysical Investigation (vertical electrical sounding)

Geophysical investigations aid in the detection of anomalous zones by measuring variations in subsurface conditions (Williams, 1997; Zhdanov and Keller, 1994; Wright, 1986). They measure certain physical properties to determine the geological sequence and structure of subsurface rocks/soils. Density, elasticity, electrical conductivity, magnetic susceptibility, and gravitational attraction are the most commonly used properties in geophysical exploration (Bell, 2007).

Table 1 CBR Adjustment Factor (Done and Samuel, 2006)

Surface moisture	The ratio of in-situ moisture to OMC (modified AASHTO)	Default CBR Adjustment Factor
Wet	1	1
Moderate	0.75	0.71
Dry	0.5	0.51
Very dry	0.25	0.37
Unknown (not assessed or difficult to assess	-	0.5

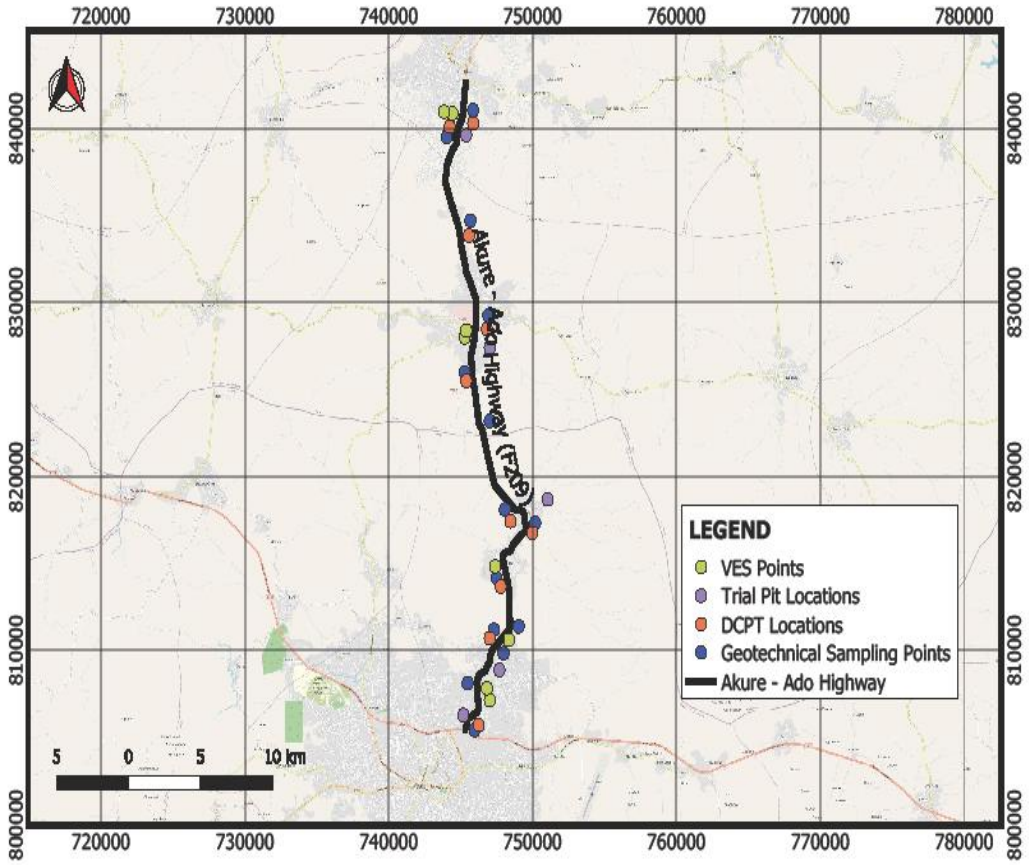

Fig. 5 Data acquisition map for the study showing the geotechnical/geochemical sampling points, geophysical locations, and trial pit points

Electrical resistivity (vertical electrical sounding) was used in this study at ten locations along the highway. An electric current is introduced into the ground via two current electrodes in this method, and the potential difference between the two potential electrodes is measured. The resist meter used in this study was capable of directly measuring apparent resistance in ohms rather than observing both current and voltage. The Schlumberger array was used at 65 m half current spacing. The obtained data (in terms of resistivity and thickness) was plotted as an apparent resistivity graph against half the current electrode separation. As a result, the electrode separation at which inflexion points appear in the graph indicates the depth/thickness of the layers' interphases and their resistivity. For data analysis involving curve fitting and modelling, the WinResist software was used. The modelling results were used to create the geoelectric section of the highway.

Fig. 6 DCPT Field Survey carried out along Akure – Ado Ekiti Highway at different locations

Trial Pits/Trenches

Five trial pits were dug along the highway to study the ground conditions, as this allows for direct assessment of weathered rocks. The holes were dug with a digger, which was repeatedly dropped into the ground. The trial pit depths are in the upper 1.0 m, and no groundwater table was discovered.

Geochemical and Geotechnical Investigation

In addition, fifteen soil samples were collected at various points along the study highway, as shown in Fig. 5. Geotechnical and geochemical tests were performed on them. The geotechnical tests were carried out using ASTM methods and procedures, and these included California Bearing Ratio (D-1883), compaction test (D-1557), particle size analysis (D-422), Atterberg limits (D-4318), moisture content (D-2216) and specific gravity (D-854; D-5550). The geochemical test was only analyzed for mineral oxides of SiO2, Fe2O3, and Al2O3 using an X-ray diffraction technique. Subsequently, the silica/sesquioxides (se) ratio was calculated to know the type of the soil and classified if laterite (se < 1.33), lateritic (1.33<se>2.0) and non-laterite (se>2.0).

Results and Discussion

Electrical resistivity geophysical survey

The summary of the VES is presented in Table 2, while the geoelectric along the highway is shown in Fig. 7. The curve types obtained from the highway alignment vary from three-layer curves i.e. H (VES 8 corresponds to Ado-Ekiti) and A (VES 5 and 6 in Ikere Ekiti) and four-layer curves KH (VESs 1-4, and 7 obtained in Akure – Igoba – Itaogbolu and Ado axis of the highway). The geological sequence underneath the pavement consists of topsoil, subsoil, a weathered layer, fracture basement (under VES 2)/fresh basement rock. The KH was the most preponderant along the pavement soil foundation, with a configuration of low resistivity overlain relatively high resistivity subsoil, followed by a weathered layer and fresh or fractured or partly weathered basement. The topsoil has resistivity ranging from 36 – 180 ohm-m (avg. 82 ohm-m) and thickness varying from 0.5 – 1.2 m (avg. 0.8 m) and is composed of clay and sandy clay (using interpretation Table 3). The average value suggests dominant clay topsoil. The subsoil delineated under VES 1 – 4 and 7 is characterized by

resistivity ranging from 135 – 711 ohm-m (avg. 385 ohm-m) composing sandy clay and clay sand (dominantly). The thickness of this layer ranged from 1.0 to 7.7 m (avg. 4.8 m). The weathered layer is clayey and has resistivity ranging between 26 ohm-m and 174 ohm-m, with a thickness of 8.8 – 40.6 m (avg. 21.6 m). The fracture basement was only observed under VES 2 with a resistivity of 829 ohm-m, while the depth to this fracture is 44.1 m. The fresh basement has resistivity ranging from 996 – 3999 ohm-m, and depths to basement rock varied from 9.9 – 36.4 m (25.3 m), indicating a thick weathering profile, especially at the southern part of the highway alignment. Consequently, the topsoil and subsoil are generally composed of clay and clay-sand soil material, which can be regarded as poor (topsoil) – good (subsoil) competent soil material to support the pavement structure. It is observed that the basement relief slopes downwardly towards the southern part. Thus since the highway sits directly on the topsoil with an average thickness of 0.8 m, it is expected the highway to fail since clay has very poor bearing capacity and high compressibility, depending on the clay activity, plasticity and clay mineralogy.

Table 2 Summary of VES results

East	North	Elevation (m)	VES NO.	Resistivity (Ohmns-meter)					Thickness (m)				Depth (m)				Curve Type
				ρ_1	ρ_2	ρ_3	ρ_4	ρ_5	h_1	h_2	h_3	h_4	d_1	d_2	d_3	d_4	
746542	806190	379	1	128	302	26	1204	-	0.6	7.7	20.0	-	0.6	8.3	28.3	-	KH
746638	806767	341	2	180	711	62	829	-	1.2	3.5	40.6	-	1.2	4.7	44.1	-	KH
748078	809743	357	3	36	340	75	3692	-	0.9	5.8	25.5	-	0.9	6.7	32.2	-	KH
747406	814064	377	4	42	135	48	996	-	0.6	5.9	29.9	-	0.6	6.5	36.4	-	KH
745870	826834	375	5	71	161	1254	-	-	1.1	8.8	-	-	1.1	9.9	-	-	A
745870	827314	380	6	73	174	1265	-	-	0.9	12.5	-	-	0.9	13.4	-	-	A
744813	839508	415	7	60	435	63	3999	-	0.5	1.0	10.6	-	0.5	1.5	12.1	-	KH
744237	839796	420	8	68	41	2568	-	-	0.8	25.2	-	-	0.8	26.0	-	-	H

Table 3 Rating of subsoil competence using Resistivity values

App. resistivity range (ohm-m)	Lithology	Competence rating
< 100	Clay	Incompetent
100 – 350	Sandy clay	Moderately competent
350 – 750	Clayey sand	Competent
> 750	Sand/Laterite/Crystalline Rock	Highly competent

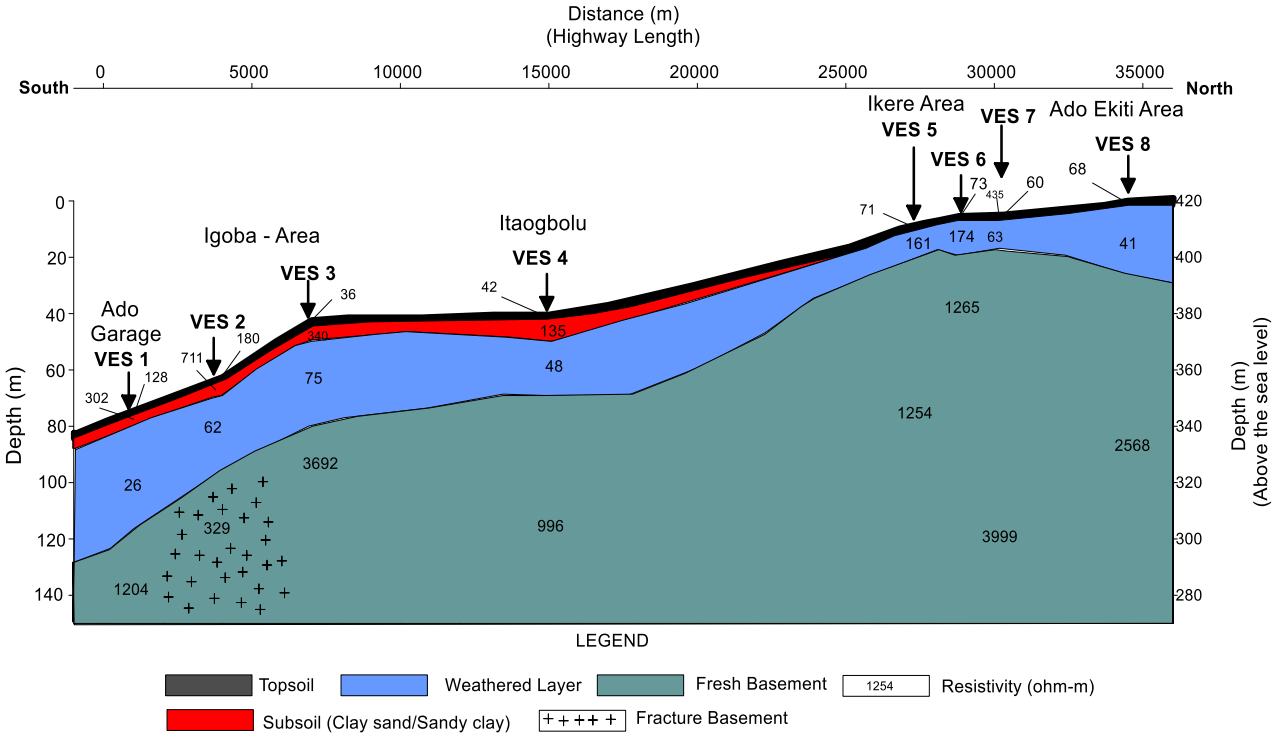

Fig. 7 Geoelectric Section along the Highway Alignment

Trial Pits

All soil types, regardless of texture, grain size, or mineralogy, can be assessed from trial pits (Vazirani and Chandola, 2009; Kezdi and Rethati, 1988). It is the most affordable method of site exploration and does not require any specialized equipment. This method involves manually excavating a pit and inspecting the soil in its natural state. The pits (Fig. 8) depict five geologic units across the pavement alignment, consisting of sandy clay, clay, clayey hardpan, sand, and lateritic sand. The upper 0.5 m is generally made up of sandy clay and clay (trial pits 01 and 02), sand, sandy clay, and clayey hardpan (trial pit 03), lateritic sand

and sandy clay (trial pits 04 and 05). Therefore the soil on which the highway is founded is dominantly sandy clay, sand and lateritic sand, which is a fair - good competent soil for civil engineering construction, including highway construction. It was observed that clayey hardpan was present in all the trial pits at a depth range of 0.25 – 1.0 m. Thus, the VES topsoil and subsoil have good agreement respectively with the trial pit section.

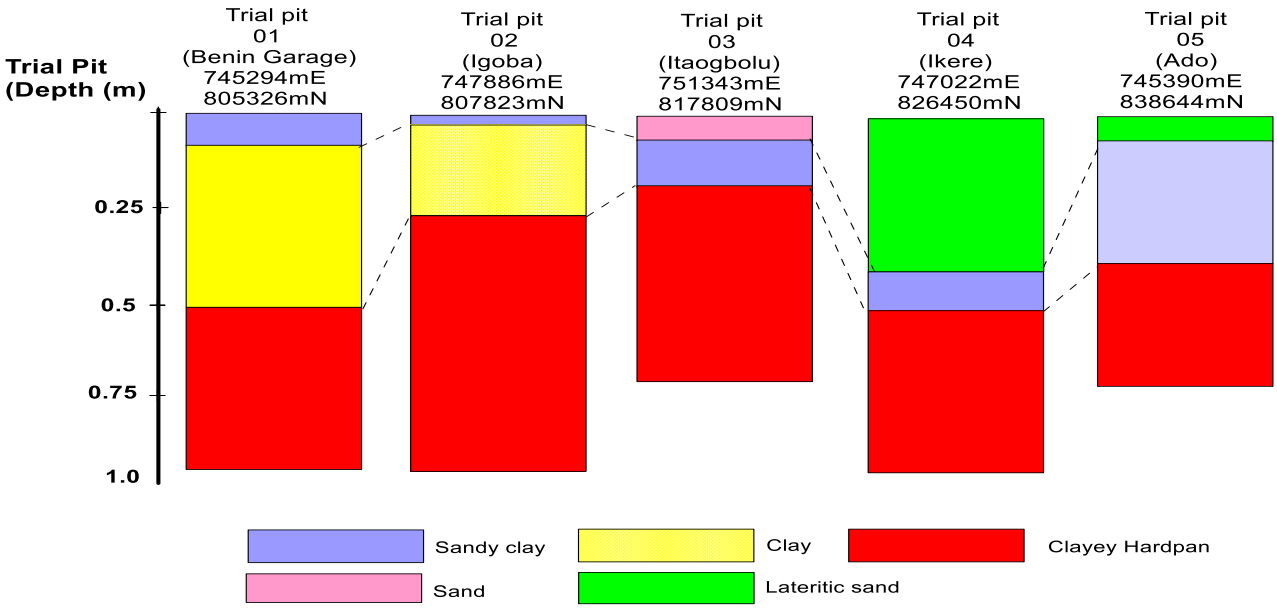

Fig. 8 Trial pit of the three sites investigated along the Highway showing the geologic section

Geochemical Analysis

The mineralogical composition of the soil influences its stability and serviceability performance. The result of the chemical analysis (oxides) of the major elements (SiO2, Fe2O3, and Al2O3) contained in the soil samples, and the silica-sesquioxide (S-S) ratio is presented in Table 4. The samples are well dominated (in descending order) by SiO2 - Al2O3 - Fe2O3, ranging from 56.62 – 63.77 % (avg. 60.37 %), 14.35 – 18.22 % (avg. 16.21 %), and 13.50–18.69 % (avg. 15.75 %) respectively. The S-S ratio of the samples ranged from 1.73 (lateritic) to 2.1 (non-laterite) (avg. of 1.90). Accordingly, soils with an S-S ratio between 1.33 and 2.0 are categorized as lateritic soil types. Therefore based on the average value of 1.90, the soils

are generally lateritic soil. This corroborates the lateritic soil observed from the trial pit sections.

Geotechnical Analysis

Table 5 presents the summary of the geotechnical laboratory and in-situ CBR results. The natural moisture content varied from 10.5 to 24.8 % (avg. 16.8 %), this range is above the 5 – 20 % acceptable range favourable for civil engineering uses or construction, but if the average value is considered, the soil still satisfied the requirement. Grain size analysis can be used to characterize the subsoil material for engineering foundation (Imeokparia and Falowo, 2020), which can serve as a guide to the engineering performance of the soil type and also provides a means by which soils can be identified quickly. The gravel and sand contents vary from 0 – 1.5 % (avg. 0.5 %) and 14.6 – 45.8 % (avg. 32.0 %) respectively. The % silt and clay contents ranged from 15.9 to 36.2 % (avg. 25.8 %) and 25.5 to 60.3 % (avg. 14.7 %). The % fines ranged from 53.2 to 84.2 (avg. 67.5). The composition of the soil is dominated (in order of magnitude) by clay, silt, and sand. The amount of % fines recorded is more than 35 % specification of the Federal Ministry of Works and Housing (1997) for highway subgrade. The plasticity chart (Fig. 9a) shows that the fines in the samples is dominated by clay of low (6.7 %) - intermediate (86.6) – high (6.7 %) plasticity/compressibility. All the soil samples are plotted above the A-line.

In terms of clay mineralogy, the soil samples are plotted within the illite (20 %) and montmorillonite (80 %) clay mineralogy group (Fig. 9b). Montmorillonite is made up of two silica sheets and one gibbsite sheet and bonded by Vander wall forces between the tops of silica sheets is weak and there's negative charge deficiency, water and exchangeable ions can enter and separate the layers. Hence montmorillonite has a very strong attraction for water and swells on the absorption of water. Illite has a similar structure similar to montmorillonite, however, in illite the interlayers are bonded together with a potassium ion linkage, making it have relatively less attraction for water. Therefore it is expected that the soil will exhibit more of montmorillonite characteristics i.e. will have a high affinity for water absorption (Bell, 1993; Attewell and Farmer, 1988). The activity ranged from 0.4 to 0.95 (avg. 0.63) signifying inactive clay type.

Table 4 Result of the Chemical analysis of three major mineral oxide

Mineral oxide	S1	S2	S3	S4	S5	S6	S7	S8	S9	S10	S11	S12	S13	S14	S15
SiO_2	59.33	62.21	60.5	56.62	60.85	61.33	59.98	63.77	60.62	58.48	63.5	60.12	59.87	60.32	58.11
Al_2O_3	15.47	15.65	13.5	16.86	17.3	14.2	15.88	14.26	16.45	13.63	15.8	18.69	15.2	17.9	15.46
Fe_2O_3	14.78	17.5	15.28	14.35	15.58	16.3	17.42	16.69	15.87	17.2	16.84	15.66	15.71	15.69	18.22
S-S ratio	1.96	1.88	2.10	1.81	1.85	2.01	1.80	2.06	1.88	1.90	1.95	1.75	1.94	1.80	1.73
Soil Type	Lateritic	Lateritic	Non-laterite	Lateritic	Lateritic	Non-laterite	Lateritic	Non-laterite	Lateritic	Lateritic	Lateritic	Lateritic	Lateritic	Lateritic	Lateritic

Table 5 Summary of the geotechnical Properties of the Investigated Soil

Parameter	S1	S2	S3	S4	S5	S6	S7	S8	S9	S10	S11	S12	S13	S14	15
East	746062	745486	748078	747310	749230	747598	747694	750382	748270	747118	745486	746830	745486	743949	745678
North	804654	807151	808735	810511	810516	813200	813200	816464	817328	822129	825010	828370	833747	838452	839988
NMC	15.1	14.9	18.7	15.6	12.1	16.6	15.5	11.3	16.5	19.5	19.6	21.2	24.8	19.6	10.5
%Gravel	0	1.5	0	0	0	1	0	0	1.2	0	1.2	0	0	1	1.2
%Sand	38.3	45.3	38.6	45.8	32.4	41.8	22.6	30.5	33.8	44.6	18.8	21.7	22.8	28.5	14.6
%Silt	36.2	27.3	25.6	22.4	34.3	17.6	32.2	29	29.9	22	24.4	28.5	16.9	15.9	24.7
%Clay	25.5	25.9	35.8	31.8	33.3	39.6	45.2	40.5	35.1	33.4	55.6	49.8	60.3	54.6	59.5
%Fines	61.7	53.2	61.4	54.2	67.6	57.2	77.4	69.5	65	55.4	80	78.3	77.2	70.5	84.2
SG	2.66	2.652	2.668	2.655	2.677	2.66	2.69	2.657	2.7	2.705	2.66	2.685	2.664	2.645	2.697
LL (%)	41.4	37.6	46.3	47.8	52.5	48.9	50.2	47.8	55.5	52.7	49.2	49.9	48.1	51.6	62.4
PL (%)	24.45	24.65	22	22.9	31.2	21.4	20.1	22.6	27.2	20.9	26.2	21	23.7	25.4	29.9
PI (%)	16.95	12.95	24.3	24.9	21.3	27.5	30.1	25.2	28.3	31.8	23	28.9	24.4	26.2	32.5
SL	10.1	10.6	8.9	8.5	10.5	7.2	8.6	9.8	11.2	10.5	10.3	9.9	10.4	8.5	12.6
CBR Lab	12	11	4	6	5	9	4	7	5	12	7	3	5	7	9
CBR Field	10	-	-	9	-	13	6	12	-	18	6	8	-	5	14
MDD	1756	1658	1722	1690	1766	1806	1662	1680	1714	1702	1636	1677	1723	1669	1723
OMC	17.3	20.5	23.3	21.5	18.8	24.6	20.1	16.3	22.4	28.6	27.1	24.4	29.8	22.2	25.7
GI	9	5	13	10	15	13	13	17	17	14	12	7	19	18	18
GI Class	Fair	Fair	Poor	Poor	Poor	Poor	Poor	Poor	Poor	Poor	Poor	Fair	Poor	Poor	Poor
Rec. Thickness (mm)	267	279	521	414	445	521	521	432	312	414	432	267	445	432	312
AASHTO	A-6	A-6	A-6	A-6	A-7-6	A-6	A-7-6	A-6	A-7-6	A-7-6	A-6	A-6	A-6	A-6	A-7-6
USCS	CL	CL	CL	CL	CH-ML	CL	CH	CL	CH	CH	CL	CL	CL	CL	CH
Subgrade Rating	Fair	Fair	Fair	Fair	Poor	Fair	Poor	Fair	Poor	Poor	Fair	Fair	Fair	Fair	Poor
Activity	0.66	0.50	0.68	0.78	0.64	0.69	0.67	0.62	0.81	0.95	0.41	0.58	0.40	0.48	0.55
Clay Type	Inactive	Inactive	Inactive	Normal	Inactive	Inactive	Inactive	Inactive	Normal	Normal	Inactive	Inactive	Inactive	Inactive	Inactive
Clay mineralogy	I	I	M	M	I-M	I-M	M	I-M	I-M	M	I-M	I-M	I-M	I-M	I-M

The specific gravity (SG) is closely related to the soil's mineralogy and/or chemical contents; the higher SG, the higher the degree of lateralization (Brown, 1996; Carter and Bentley, 1991)). In addition, the larger the clay fraction and alumina contents, the lower is the SG. The values of specific gravity of the samples ranged between 2.645 – 2.705 (avg. 2.672). The standard range of value of specific gravity of soils for civil engineering construction lies between 2.60 and 2.80 (Daramola et al., 2015; Ademeso and Ogunjobi, 2021), these values are considered normal for civil engineering construction; hence the soils are competent. Specific gravity is known to correlate with the mechanical strength of soil and may be used as a basis for selecting suitable highway pavement construction materials particularly when used with other pavement construction materials. The liquid limit (LL) values ranged between 37.6 to 62.4 % (avg. 49.5 %), plastic limits (PL) ranged between 20.1 to 31.2 % (avg. 24.2 %) and plasticity index (PI) between 12.95 to 32.5 % (avg. 25.2 %). The Federal Ministry of Works and Housing recommends LL of 50% (max.), PI of 20% (max.), plastic limit of 30 % (max.) and % fines of 35 maximum for highway subgrade soil. Soil with high LL, PL, and PI is usually characterized by low bearing pressure. Hence the soils do not satisfy the requirement of PI as subgrade material. The linear shrinkage (SL) ranged between 7.2 to 12.6 % (avg. 9.8 %), signifying a moderately high swelling potential, even though SL greater than 8.0 tends to be active, of critical swelling potential.

Compaction is concerned with the interactions of moisture content, applied effort, and density. On the road, compaction is performed to increase mass density and thus the strength, rigidity, and durability of placed materials (Bell, 2007). Compaction testing is performed in the laboratory to predict moisture density responses of a material to applied effort and to provide a reference for controlling on-site compaction during construction (Bell, 2004). The maximum dry density (MDD) for the soil samples varied between 1636 and 1806 kg/m3 (1705 kg/m3) at standard proctor compaction energy while the optimum moisture content (OMC) ranged between 16.3 and 29.8 % (22.8 %). An important part of the grading of the site often includes the compaction of fill. All the soil samples have moderately high MDD at moderately high OMC.

The California Bearing Ratio (CBR) is an empirical test used in road engineering to determine the strength and rigidity of compacted material at a given level of compaction

(Brown, 1996). All compacted samples show soaked CBR values ranging between 3 and 12 % (avg. 7 %), with corresponding in-situ values obtained from DCPT ranging from 5 to 18 % (avg. 10 %). The Federal Ministry of Works and Housing recommends a California Bearing Ratio of greater than 10% for subgrade materials. Therefore using Table 8, the soils are rated as low (based on average value) as pavement subgrade material. The GI values obtained ranged from 5 to 19 (avg. 13) corresponding to poor subgrade soil. The result shows that the California Bearing Ratio values of the soils both in-situ and laboratory do not satisfy the 10 % minimum specification. Using Table 6, the soil can be regarded as subgrade soil with medium strength classification.

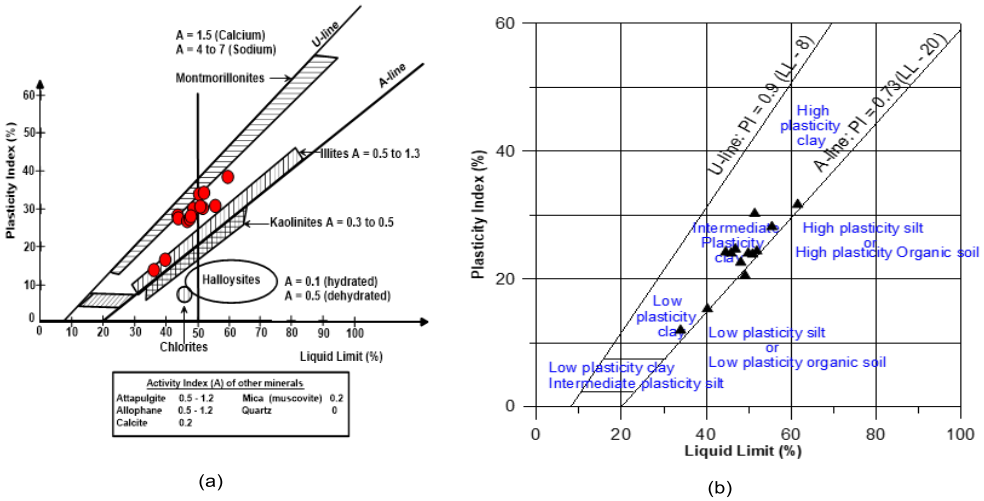

Fig. 9 (a) Plasticity Chart for Fine Contents of the soil samples (b) Clay mineralogy group of the soil samples with most within/or near the illite

Based on the GI and CBR values, and the traffic count carried out which placed the highway as Class-E, the recommended thickness (Fig. 10) of the basement should range from 267 mm (good segment) to 521 mm (for weak segment) (avg. 401 mm). This recommended thickness is far above the obtainable value of 159 – 210 mm, measured along the highway structure (Fig. 11). This implies that the highway is a thickness deficit, which may be the cause of the failure of the pavement structure. Therefore the present design thickness of the highway will not be able to sustain the vehicular loads/haulage activities on the highway.

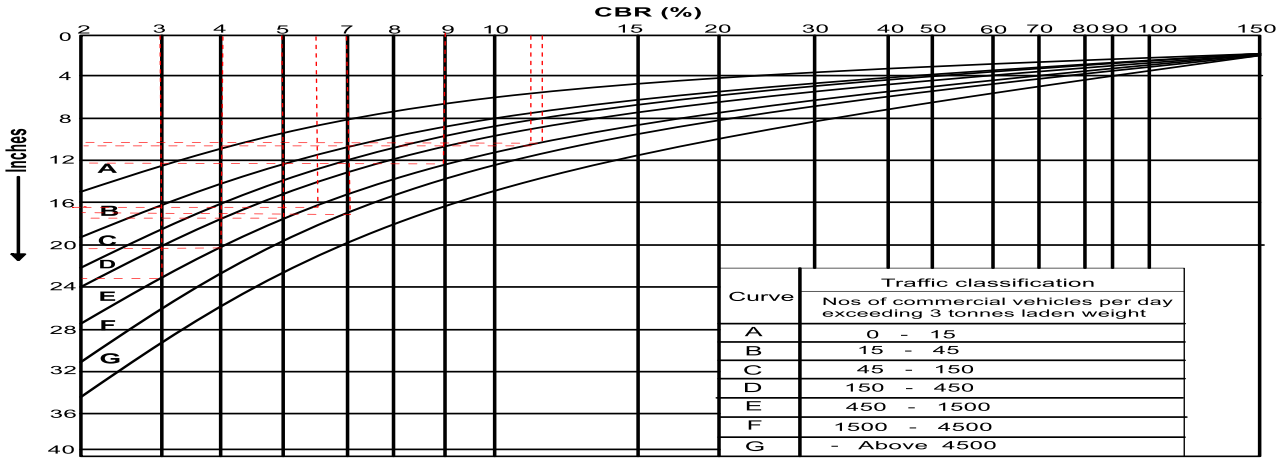

Fig. 10 The CBR Chart adopted for determine the recommended thickness across the highway alignment

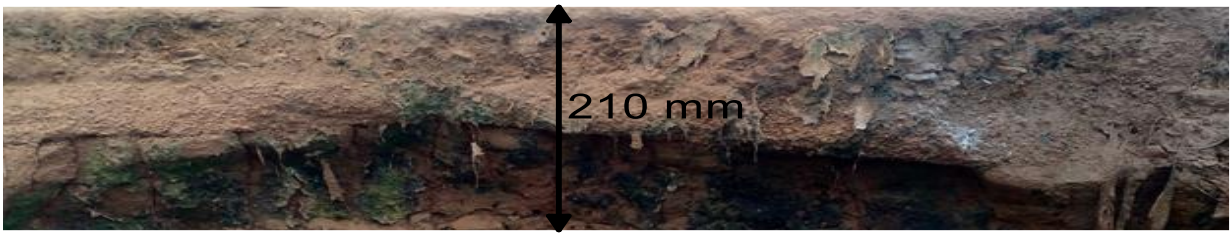

Fig. 11 Existing Design Thickness of 210 mm measured at an exposed section of the structural layers between Igoba and Itaogbolu

DCPT Analysis

The result summary of the DCPT results is presented in Table 7, while subsoil layering concerning its depth and in-situ CBR is shown in Figs 12 and 13. In Table 7, the degree of penetration ranged from 715 mm (Site 2) – 965 mm (Test 10), with a cumulative number of blows ranging from 24 (Sites 7 and 8) to 60 (Site 4). The penetrative index or rate ranged between 1.60 mm/blow (Site 5 at a penetration depth of 751 mm) – 97.67 mm/blow (Site 7 at a penetration depth of 597 mm). All the tests are characterized by a low - moderate cumulative number of blows in the upper 1 m investigated, signifying a generally loose - medium consistencies of relative densities of 0.320 to 0.440 (Table 8); and for every 10cm, the number of blows recorded varied from 3 - 5 with equivalent CBR of 6 – 10 % and penetrative index of 30 – 20 mm/blow (using Table 9 interpretation). In addition, the upper 500 mm is loose, it is very critical at Site 8, only the depths 10 – 20 cm are of medium

consistency of RD of 0.389. Concerning layering, it varied from two layers observed at Sites 1 – 9 to three layers observed at Site 10. The obtained CBR ranged from 4 % at Sites 7 and 8 with respective penetration depth/thickness of 930 mm/789 and 927 mm/769 mm to 32 % at Site 1 with penetration depth/thickness of 717 mm/90 mm. The most competent layers in terms of the obtained CBR are 141 mm (Site 7) to 738 mm (Site 6).

Table 6 Subgrade strength classification for the studied highway (Carter and Bentley, 1991)

Soaked CBR	Strength classification	Comments
< 1%	Extremely weak	Geotextile reinforcement and separation layer with a working platform typically required
1 % - 2 %	Very weak	Geotextile reinforcement and/or separation layer and/or a working platform typically required
2 % - 3 %	Weak	Geotextile separation layer and/or a working platform typically required
3 % - 10 %	Medium	
10 % - 30 %	Strong	Good subgrades to sub-base quality material
>30%	Extremely strong	Sub-base to base quality material

Table 7 Summary of the DCPT showing the penetrative rate, depth of penetration, and number of blows for all the ten locations along the highway

SITE 1: EAST: 746158m; NORTH: 804750m; CH. 0 + 0.001 RHS																
Blow	0	3	3	3	3	3	3	3	3	4	4	4	-	-	-	-
Penetration (mm)	32	108	170	272	349	429	512	581	660	711	731	750	-	-	-	-
Cum. Blows	0	3	6	9	12	15	18	21	24	28	32	36	-	-	-	-
Depth (mm)	0	75	137	239	316	396	479	548	627	678	698	717	-	-	-	-
Penetration rate (mm/blow)	0	25.0	20.67	34.0	25.67	26.67	27.67	23.0	26.33	12.75	5.0	4.75	-	-	-	-
SITE 2: EAST: 747022m; NORTH: 809935m; CH. 0 + 6.2 LHS																
Blow	0	3	3	3	3	3	3	3	3	4	4	4	-	-	-	-
Penetration (mm)	33	94	155	238	305	389	472	544	623	671	692	715	-	-	-	-
Cum. Blows	0	3	6	9	12	15	18	21	24	28	32	36	-	-	-	-
Depth (mm)	0	62	123	206	273	357	440	512	591	639	660	679	-	-	-	-
Penetration rate (mm/blow)	0	20.67	20.33	27.67	22.33	28.0	27.67	24.0	26.33	16.0	7.0	4.75	-	-	-	-
SITE 3: EAST: 747694m; NORTH: 812528m CH. 0 + 9.3 LHS																
Blow	4	4	4	4	4	4	4	5	5	5	5	5	5	2	2	-
Penetration (mm)	28	85	135	172	221	260	299	342	390	461	541	631	830	920	950	-
Cum. Blows	0	4	8	12	16	20	24	29	34	39	44	49	54	56	58	-
Depth (mm)	0	57	107	144	193	232	271	314	362	433	513	603	802	892	922	-
Penetration rate (mm/blow)	0	14.25	12.50	9.25	12.25	9.75	9.75	8.60	9.60	14.20	16.0	18.0	39.80	18.0	6.0	-
SITE 4: EAST: 749710m; NORTH: 815792m; CH. 0 + 12.5 RHS																
Blow	0	4	4	4	4	4	4	5	5	5	5	5	5	2	2	2
Penetration (mm)	30	72	123	169	218	253	284	310	369	432	501	592	744	843	938	950
Cum. Blows	0	4	8	12	16	20	24	29	34	39	44	49	54	56	58	60
Depth (mm)	0	42	93	139	188	223	254	280	339	402	471	562	714	813	908	920
Penetration rate (mm/blow)	0	10.50	12.75	11.50	12.25	8.75	7.75	5.20	11.80	12.60	13.80	18.20	30.40	49.50	47.50	6.0
SITE 5: EAST: 748558m; NORTH: 816368m; CH. 0 + 13.9 LHS																
Blow	0	3	3	3	3	3	3	3	5	5	5	5	5	-	-	-
Penetration (mm)	20	65	105	185	341	455	501	537	592	640	691	722	739	-	-	-
Cum. Blows	0	3	6	9	12	15	18	21	26	31	36	41	46	-	-	-
Depth (mm)	0	45	85	165	321	435	481	517	572	620	671	702	719	-	-	-
Penetration rate (mm/blow)	0	15.0	13.33	26.67	52.0	38.0	15.33	12.0	11.0	9.60	10.20	6.20	3.40	-	-	-
SITE 6: EAST: 745486m; NORTH: 824434m; CH. 0 + 21.9 LHS																
Blow	0	3	3	3	3	3	3	3	5	5	5	5	5	5	-	-
Penetration (mm)	22	76	114	192	376	487	532	569	624	655	708	743	751	760	-	-
Cum. Blows	0	3	6	9	12	15	18	21	26	31	36	41	46	51	-	-
Depth (mm)	0	54	92	170	354	465	510	547	602	633	686	721	729	738	-	-
Penetration rate (mm/blow)	0	18.0	12.67	26.0	61.33	37.0	15.0	12.33	11.0	6.20	10.60	7.0	1.60	1.80	-	-
SITE 7: EAST: 746638m; NORTH: 827602m; CH. 0 + 24.4 RHS																

Blow	0	3	3	3	3	3	3	3	2	-	-	-	-	-	-	-
Penetration (mm)	35	105	115	176	304	597	723	900	956	-	-	-	-	-	-	-
Cum. Blows	0	3	6	9	12	15	18	21	24	-	-	-	-	-	-	-
Depth (mm)	0	70	80	141	269	562	688	865	930	-	-	-	-	-	-	-
Penetration rate (mm/blow)	0	23.33	3.33	20.33	42.67	97.67	42.0	59.0	21.67	-	-	-	-	-	-	-
SITE 8: EAST: 745678m; NORTH: 832883m; CH. 0 + 30.0 RHS																
Blow	0	3	3	3	3	3	3	3	2	1	-	-	-	-	-	-
Penetration (mm)	34	99	143	192	328	623	757	882	955	961	-	-	-	-	-	-
Cum. Blows	0	3	6	9	12	15	18	21	23	24	-	-	-	-	-	-
Depth (mm)	0	65	109	158	294	589	723	848	921	927	-	-	-	-	-	-
Penetration rate (mm/blow)	0	21.67	14.67	16.33	45.33	98.33	44.67	41.67	36.50	6.0	-	-	-	-	-	-
SITE 9: EAST: 744333m; NORTH: 839316m; CH. 0 + 36.2 LHS																
Blow	0	3	3	3	3	3	3	3	3	3	3	3	5	5	3	-
Penetration (mm)	25	74	104	140	188	235	265	300	342	395	425	465	630	810	949	-
Cum. Blows	0	3	6	9	12	15	18	21	24	27	30	33	38	43	46	-
Depth (mm)	0	49	79	115	163	210	240	275	317	370	400	440	605	785	924	-
Penetration rate (mm/blow)	0	16.33	10.0	12.0	16.0	15.67	10.0	11.67	14.0	17.67	10.0	13.33	33.0	36.0	46.33	-
SITE 10: EAST: 746062m; NORTH: 839316m; CH. 0 + 36.7 RHS																
Blow	0	3	3	3	3	3	3	3	3	3	3	3	5	5	3	-
Penetration (mm)	26	82	112	156	204	266	291	328	361	402	438	473	655	838	965	-
Cum. Blows	0	3	6	9	12	15	18	21	24	27	30	35	40	43	46	-
Depth (mm)	0	56	86	130	178	240	265	302	335	376	412	447	629	812	939	-
Penetration rate (mm/blow)	0	18.67	10.0	14.67	16.0	20.67	8.33	12.33	11.0	13.67	12.0	11.67	36.40	36.60	42.33	-

From the values, the strength coefficient is also generally low for subbase and base material. Resilient modulus (MR) is a measure of subgrade material stiffness. It is a means of estimating the modulus of elasticity (ER) of rapidly applied loads as against the slowly applied load used for ER. The Young modulus (ER) and resilient modulus (MR) were estimated by Lockwood et al. (1992), Jianzhou et al. (1999), and George and Uddin (2000); and the ER varied between 5.94 – 549.41 (avg. 167.516), 59.19 – 240.44 (avg. 138.957), and 23.81 – 155.2 (avg. 78.957); the MR ranged from 19.01 to 597.82 (avg. 191.095), 75.72 to 268.76 (avg. 160.679), and 38.05 to 177.98 (avg. 96.779) respectively (Table 10). Lockwood et al. (1992) and Jianzhou et al. (1999) showed closely overlapping average values, while George and Uddin (2000) showed a wide variation (Table 10) in the values of ER and MR.

Table 8 Typical DCP-CBR relationship (Carter and Bentley, 1991)

Blows/100 mm	In situ CBR (%)	mm/blow
<1	<2	>100 mm
1-2	2-4	100-50 mm
2-3	4-6	50-30 mm
3-5	6-10	30-20 mm
5-7	10-15	20-15 mm
7-10	15-25	15-10 mm
10-15	25-35	10- mm
15-20	35-50	7-5 mm
20-25	50-60	5-4 mm
>25	>60	<4 mm

Parameters modelling and correlations

The obtained soaked CBR from the laboratory was correlated with in-situ CBR obtained from the processing of DCPT data, the plot gives a weak positive correlation coefficient (R2) of 0.4445 (Fig. 13a), and linear regression model (equation 10):

$$\text{CBR (in-situ)}=0.9254x+3.0672 \quad (10)$$

In this relationship, x = CBR (soaked)

The relative density (RD) values obtained from "DIN 4094" equation was plotted against in-situ CBR and DCPI. This gives a regression model of equations 11 and 12, with strong and weak positive correlations (R2) of 0.7925 and 0.4255 respectively (Fig. 13b and c).

$$\text{CBR (in-situ)} = 0.18871e10.059x \quad (11)$$

$$\text{DCPI} = -135.4\ln(x) - 126.58 \quad (12)$$

In these relationships, x = relative density

Table 9 DCPT results showing relative densities per every 10 cm, their penetrative rate, and the consistencies of the soil

	TEST 1								
Depth (cm)	10	20	30	40	50	60	70	80	90
Blows per 10cm	3	3	3	3	3	3	4	4	4
Relative Density	0.320	0.320	0.320	0.320	0.320	0.320	0.348	0.348	0.348
Soil Consistency	Loose	Loose	Loose	Loose	Loose	Loose	Medium	Medium	Medium
Penetration rate (mm/blow)	25	20.67	34.0	-	26.67	27.67	12.75	4.75	-
	TEST 2								
Depth (cm)	10	20	30	40	50	60	70	80	90
Blows per 10cm	3	3	3	3	3	4	4	4	4
Relative Density	0.320	0.320	0.320	0.320	0.320	0.348	0.348	0.348	0.348
Soil Consistency	Loose	Loose	Loose	Loose	Loose	Medium	Medium	Medium	Medium
Penetration rate (mm/blow)	20.67	-	22.33	-	-	-	4.75	-	-
	TEST 3								
Depth (cm)	10	20	30	40	50	60	70	80	90
Blows per 10cm	4	4	4	5	10	5	10	4	6
Relative Density	0.348	0.348	0.348	0.371	0.440	0.371	0.440	0.348	0.389
Soil Consistency	Loose	Loose	Loose	Medium	Medium	Medium	Medium	Loose	Medium
Penetration rate (mm/blow)	13.50	12.25	-	9.60	-	-	-	-	18.0
	TEST 4								
Depth (cm)	10	20	30	40	50	60	70	80	90
Blows per 10cm	4	4	4	5	10	5	10	6	6
Relative Density	0.348	0.348	0.348	0.371	0.440	0.371	0.440	0.389	0.389
Soil Consistency	Loose	Loose	Loose	Loose	Loose	Medium	Medium	Medium	Medium
Penetration rate (mm/blow)	12.75	12.75	5.20	-	13.80	18.20	-	-	-
	TEST 5								
Depth (cm)	10	20	30	40	50	60	70	80	90
Blows per 10cm	3	3	3	3	5	5	5	5	5
Relative Density	0.320	0.320	0.320	0.320	0.371	0.371	0.371	0.371	0.371
Soil Consistency	Loose	Loose	Loose	Loose	Medium	Medium	Medium	Medium	Medium
Penetration rate (mm/blow)	13.3	-	-	-	15.33	11.0	-	-	-
	TEST 6								
Depth (cm)	10	20	30	40	50	60	70	80	90
Blows per 10cm	3	3	3	3	3	5	5	5	-
Relative Density	0.320	0.320	0.320	0.320	0.320	0.371	0.371	0.371	-
Soil Consistency	Loose	Loose	Loose	Loose	Loose	Medium	Medium	Medium	-
Penetration rate (mm/blow)	12.67	23.0	-	-	-	11.0	10.6	-	-
	TEST 7								
Depth (cm)	10	20	30	40	50	60	70	80	90
Blows per 10cm	3	3	3	6	6	6	6	3	6
Relative Density	0.320	0.320	0.320	0.389	0.389	0.389	0.389	0.320	0.389
Soil Consistency	Loose	Loose	Loose	Medium	Medium	Medium	Medium	Loose	Medium
Penetration rate (mm/blow)	23.33	-	42.67	-	-	-	-	-	59.0
	TEST 8								
Depth (cm)	10	20	30	40	50	60	70	80	90
Blows per 10cm	3	6	3	3	3	3	3	3	3
Relative Density	0.320	0.389	0.320	0.320	0.320	0.320	0.320	0.320	0.320
Soil Consistency	Loose	Medium	Loose	Loose	Loose	Loose	Loose	Loose	Loose
Penetration rate (mm/blow)	21.67	-	44.30	-	-	-	-	-	38.50
	TEST 9								
Depth (cm)	10	20	30	40	50	60	70	80	90
Blows per 10cm	3	3	3	3	3	5	5	5	3
Relative Density	0.320	0.320	0.320	0.320	0.320	0.371	0.371	0.371	0.320
Soil Consistency	Loose	Loose	Loose	Loose	Loose	Medium	Medium	Medium	Loose
Penetration rate (mm/blow)	10.0	-	11.67	17.67	-	-	-	36.0	-

	TEST 10								
Depth (cm)	10	20	30	40	50	60	70	80	90
Blows per 10cm	3	3	3	3	3	6	3	6	3
Relative Density	0.320	0.320	0.320	0.320	0.320	0.371	0.320	0.371	0.320
Soil Consistency	Loose	Loose	Loose	Loose	Loose	Medium	Loose	Medium	Loose
Penetration rate (mm/blow)	10.0	16.0	8.35	13.67	-	-	-	-	39.50

The relationship between ER derived from "DIN 4094" and average MR calculated from expressions proposed by Lockwood et al. (1992), Jianzhou et al. (1999), and George and Uddin (2000) is shown by the regression model in equation 13, with R2 of 0.8627 (Fig. 13d).

$$M_R = 107.77 \ln (x) - 348.57 \quad (13)$$

Where x is the modulus of elasticity.

The correlation between in-situ CBR and average MR derived from the expressions of Lockwood et al. (1992), Jianzhou et al. (1999), and George and Uddin (2000) to give equation 14, with a positive correlation coefficient of 0.5841 (Fig. 13e); while the plots of the in-situ CBR against each of this respective authors give R2 of 0.5592, 0.5855, and 0.5920 (Fig. 13f). All the models follow the same trend. The variation in the coefficients is marginal as all showed strong positive correlations. The model expressions for these relationships are presented in equations 15 – 17.

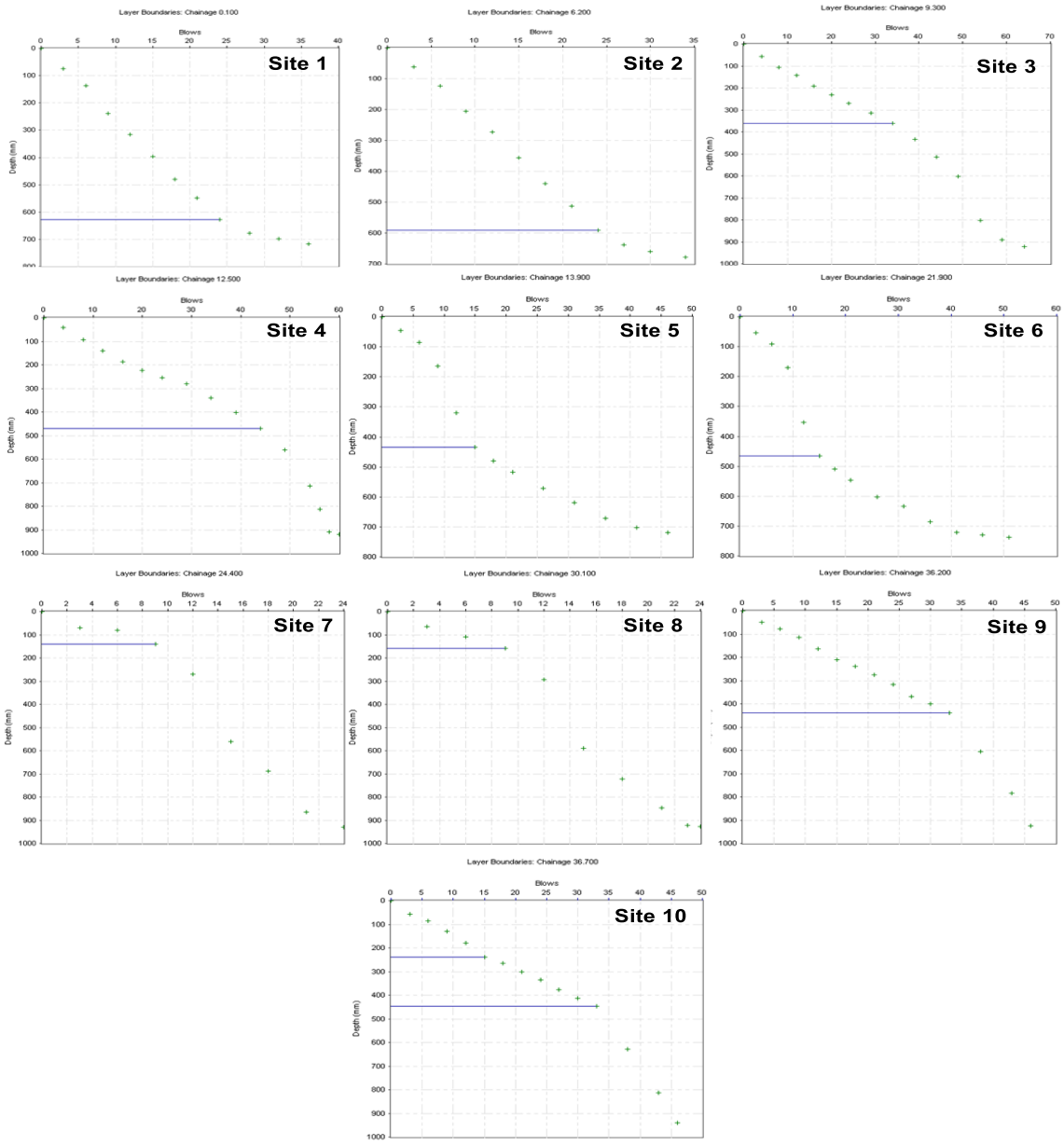

Fig. 12 The plot of Cumulative Blows against Depth at Sites (Test points) 1 – 10 showing the layering

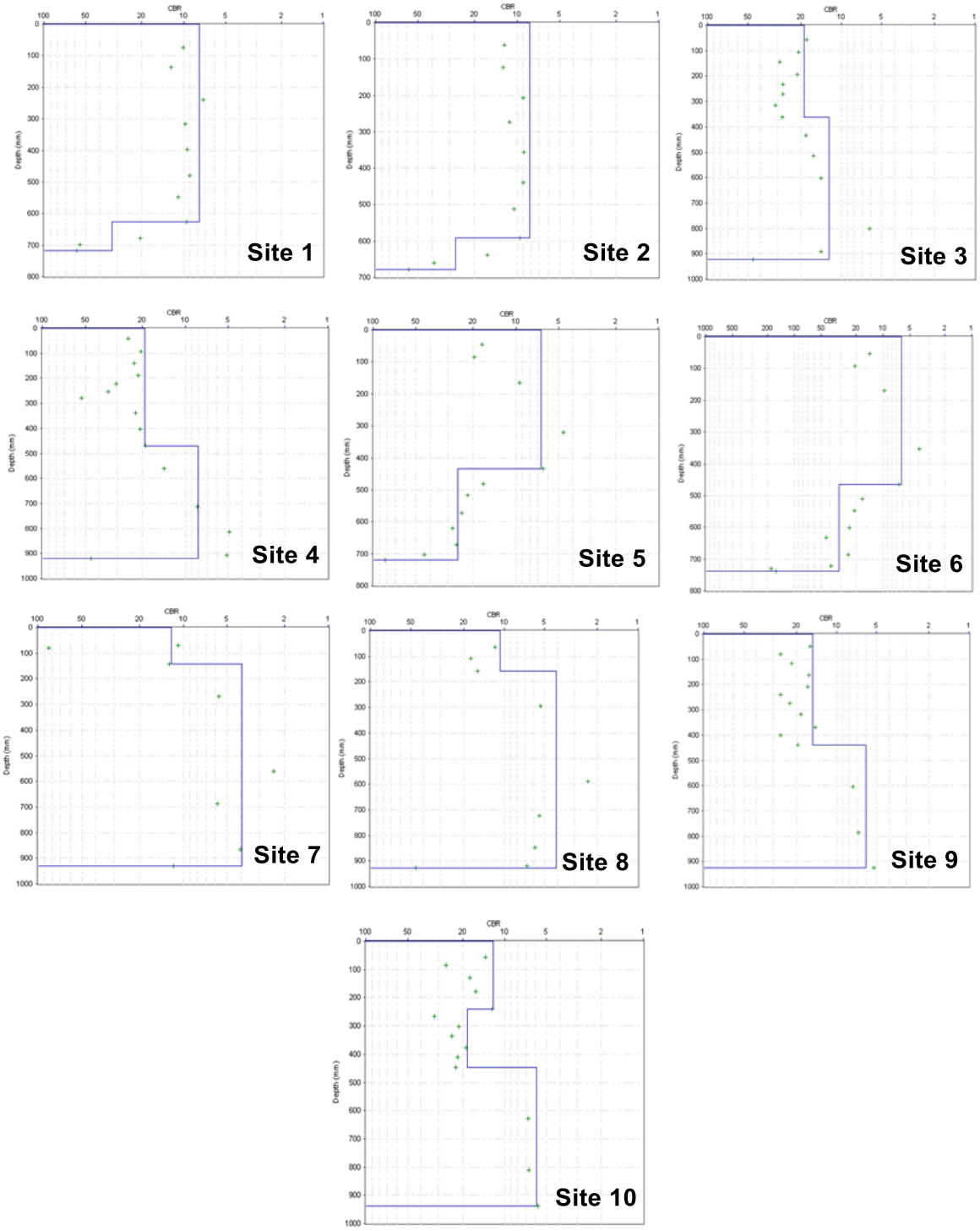

Fig. 13 The plot of CBR against Depth at Sites (Test points) 1 – 10, showing the CBR of the layers

Table 10: Summary of the CBR results in relation to strength coefficient of the soils as subgrade, subbase, and base material

Site No.	Test Layer No.	CBR (%)	Thickness (mm)	Depth (mm)	Subgrade	Position	Strength coefficient	Pavement Strength/Layer contribution			Position	Strength coefficient	Pavement Strength/Layer contribution		
					SNG			SN	SNC	SNP			SN	SNC	SNP
1	1	8	627	627	0.20	Sub-Base	0.05	1.67	1.67	1.19	Base	0.02	0.79	0.79	0.79
	2	32	90	717	1.29	Sub-Base	0.10				Base	0.08			
2	1	8	591	591	0.20	Sub-Base	0.06	1.63	1.63	1.21	Base	0.02	0.75	0.75	0.75
	2	27	88	679	1.16	Sub-Base	0.10				Base	0.07			
3	1	19	362	362	0.88	Sub-Base	0.09	2.85	2.85	1.92	Base	0.05	1.41	1.41	1.41
	2	12	560	922	0.52	Sub-Base	0.07				Base	0.03			
4	1	19	471	471	0.88	Sub-Base	0.09	2.61	2.61	1.85	Base	0.05	1.30	1.30	1.30
	2	8	449	920	0.20	Sub-Base	0.06				Base	0.02			
5	1	7	435	435	0.10	Sub-Base	0.05	1.87	1.87	1.25	Base	0.02	1.01	1.01	1.01
	2	25	284	719	1.10	Sub-Base	0.10				Base	0.06			
6	1	6	465	465	-0.02	Sub-Base	0.04	1.87	1.87	1.22	Base	0.02	1.11	1.11	1.11
	2	31	273	738	1.27	Sub-Base	0.10				Base	0.07			
7	1	12	141	141	0.52	Sub-Base	0.07	0.99	0.99	0.77	Base	0.03	0.53	0.53	0.53
	2	4	789	930	-0.34	Sub-Base	0.02				Base	0.01			
8	1	11	158	158	0.45	Sub-Base	0.07	1.05	1.05	0.80	Base	0.03	0.53	0.53	0.53
	2	4	769	927	-0.34	Sub-Base	0.02				Base	0.01			

9	1	15	440	440		Sub-Base	0.08	2.18	2.18	1.59	Base	0.04	1.01	1.01	1.01
					0.70										
	2	6	484	924		Sub-Base	0.04				Base	0.02			
					-0.02										
	10	1	12	240	240		Sub-Base	0.07	2.17	2.17	1.56	Base	0.03	1.01	1.01	1.01
						0.52										
		2	18	207	447		Sub-Base	0.09				Base	0.05			
						0.84										
		3	6	492	939		Sub-Base	0.04				Base	0.02			
						-0.02										

Table 11: Summary of the Modulus of Elasticity and Resilient Modulus at every Chainage where samples were taken

Test No.	Chainage along Highway	In situ CBR	Young modulus using Lockwood et al. (1992) M_R values	Young modulus using Jianzhou et al. (1999) M_R values	Young modulus using George and Uddin (2000) M_R values	Resilient modulus by Lockwood et al. (1992)	Resilient modulus by Jianzhou et al. (1999)	Resilient modulus by George and Uddin (2000)
Test No. 1	CH. 0+0.001RHS	32	188.44	160.93	93.49	213.38	184.08	112.25
Test No. 2	CH. 0+ 6.2LHS	27	188.44	160.93	93.49	213.38	184.08	112.25
Test No. 3	CH. 0+9.3LHS	12	144.43	145.88	82.41	166.51	168.05	100.46
Test No. 4	CH. 0+12.5RHS	8	144.43	145.88	82.41	166.51	168.05	100.46
Test No. 5	CH. 0+13.9LHS	25	273.83	185.00	111.63	304.32	209.72	131.57
Test No. 6	CH. 0+21.9LHS	31	549.41	240.44	155.20	597.82	268.76	177.98
Test No. 7	CH. 0+24.4RHS	4	28.08	83.71	39.34	42.59	101.84	54.59
Test No. 8	CH. 0+30.0RHS	4	144.43	145.88	82.41	166.51	168.05	100.46
Test No. 9	CH. 0+36.2LHS	6	5.94	59.19	23.81	19.01	75.72	38.05
Test No. 10	CH. 0+36.7RHS	6	7.73	61.73	25.38	20.92	78.44	39.72

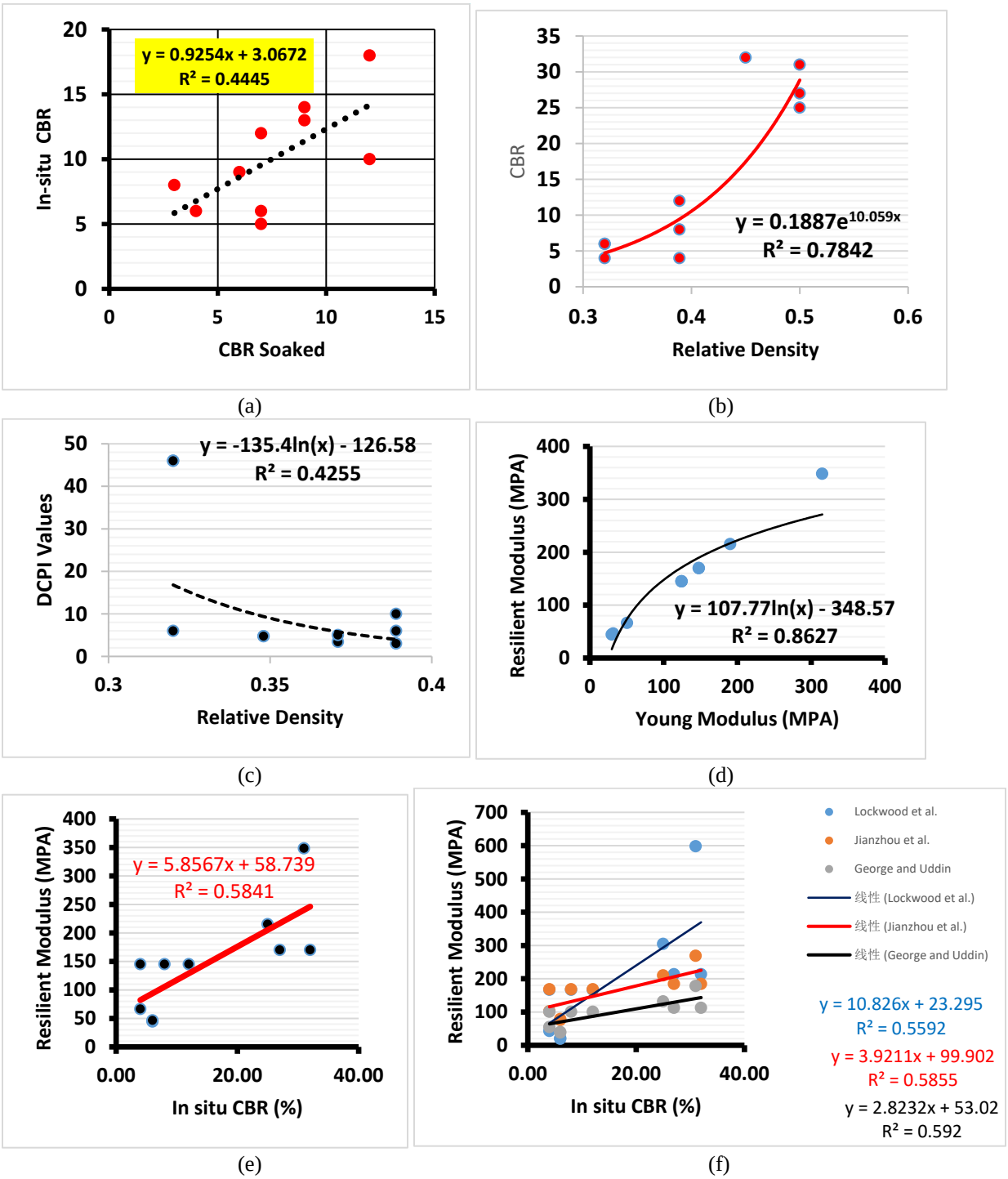

Fig. 14 Regression models for (a) CBR lab and in-situ CBR (b) RD and in-situ CBR (c) RD and DCPI (d) ER and MR (e) in-situ CBR and MR (f) in-situ and MR for Lockwood et al. (1992), Jianzhou et al. (1999), and George and Uddin (2000)

$$M_R = 5.8567x + 58.739 \quad (14)$$

$$M_R = 10.826x + 23.295 \quad (15)$$

$$M_R = 3.9211x + 99.902 \quad (16)$$

$$M_R = 2.8232x + 53.020 \quad (17)$$

Conclusion

As a result, it is possible to conclude that the highway is founded on clay, sandy clay, sand, and lateritic sand, which is a poor to good competent soil for civil engineering construction, including highway construction. Clayey hardpan was found in all of the trial pits at depths ranging from 0.25 to 1.0 m. The S-S ratio averages 1.90, and the soils are predominantly lateritic. This supports the lateritic soil observed in trial pit sections. The geotechnical properties revealed that the SC-SM classification is dominated by clay soil (41.7%), sand (32.5%), and silt (25.8%). The percentage of fines recorded exceeds the 35% limit set by the Federal Ministry of Works and Housing (1997) for highways subgrade. The plasticity chart shows that the fines in the samples is dominated by the clay of low (6.7 %) - intermediate (86.6) – high (6.7 %), with montmorillonite (80 %) clay mineralogy group. Although the clay activity value of 0.63 avg. suggests inactive soil type. The soaked CBR values (avg. 7 %), with corresponding in-situ values (avg. 10 are less than 10% minimum specification for subgrade materials. The GI values obtained have a value of 13 corresponding to poor subgrade soil. Based on the GI and CBR values, and the traffic count carried out which placed the highway as Class-E, the recommended thickness of the basement should range from 267 mm (good segment) to 521 mm (for weak segment) (avg. 401 mm). Thus, these recommended thicknesses are far above the measurement carried out in the field along the highway structure of 159 – 210 mm. This implies that the highway is a thickness deficit, which may be the cause of the incessant pavement structure failure. Therefore, the present design thickness of the highway will not be able to sustain the vehicular loads/haulage activities on the highway.

All the DCPT test sites are characterized by a low - moderate cumulative number of blows in the upper 1 m investigated, signifying a generally loose - medium consistencies of relative densities of 0.320 to 0.440. Nonetheless, the range of values or average is less than

0.5 SNG strength coefficient for the subgrade pavement layer. In addition, a negative strength coefficient was recorded in the last five chainages representing a very weak soil domain. The penetrative index or rate ranged between 1.60 mm/blow (Site 5 at a penetration depth of 751 mm) – 97.67 mm/blow (Site 7 at a penetration depth of 597 mm). In addition, the upper 500 mm is loose, it is very critical at Site 8, only the depths 10 – 20 cm are of medium consistency of RD of 0.389. The SNG contribution of the soil as subgrade material (avg. 0.48), strength coefficient of the soil as subbase (avg. 0.0671) and base (avg. 0.0357), in terms of SN/SNC and SNP are less than 0.5 minimum required for pavement strength/layer contribution. Therefore, the highway failure can be attributed to weak engineering properties, coupled with inadequate design thickness Also lack of drainage facility at the shoulders of the highway could have also contributed. The expansion and shrinking, collapse, and dispersal associated with clayey soil can very problematic, hence the soil beneath the highway should be stabilized (instead of total removal due to its thickness) with lime or the addition of coarse soil particles before reconstruction to minimize the degree of shrinkage and swelling they could undergo.

Acknowledgements:

The author is grateful to TETFund, Nigeria (under the Institution Based Research) Nigeria. Special appreciation to all students of the Civil Engineering Technology Department for the assistance rendered during data acquisition.

Funding

No funding was received by the author for conducting the study.

Declaration

Conflict of interest: The author declares that he has no conflict of interest with anyone in the writing and publication of this study.

Data Availability Statement

All data generated or analyzed during this study are included in this published article [and its supplementary information files].

Author Contribution

The author designed the study, acquired, analyzed, and interpreted the data. He also drafted the work and approved the revision to be published.

References

Ademeso, O. A., and Ogunjobi, O. S. 2021. Hydraulic Conductivity of Subsoils vis-à-vis Foundation Applications in Akure, Southwestern Nigeria. Journal of Mining and Geology 57(1), pp 217-224

Adetoro, A. E., and Abe, O. E. 2018. Assessment of Engineering Properties of Ado-Ekiti to Ikere-Ekiti Road Soil, Southwestern Nigeria. World Wide Journal of Multidisciplinary Research and Development, 4(6): 191-195

Anon, 1952. Soil Mechanics for Road Engineers Transport and Road Research Laboratory, Her Majesty's Stationery Office, London

ASTM D4318-10, 2010. Standard test method for liquid limit, and plasticity index of soils.American Society for Testing and Materials.

ASTM D698, 2015. Standard Test Method for laboratory compaction characteristics of soil using standard effort. American Society for Testing and Materials

ASTM D6951-3, 2003. Standard Test Method for Use of the Dynamic Cone Penetrometer in Shallow Pavement Applications.

ASTM D6913-04, 2009. Standard test method for particle size analysis of soil. American Society for Testing and Materials.

ASTM D4429-09, 2009. Standard test method for CBR (California Bearing Ratio) of Soils.American Society for Testing and Materials.

ASTM D 2216, 2015. Standard Test Method for laboratory moisture content determination of soil using American Society for Testing and Materials.

ASTM D 698, 2010. Standard Test Method for laboratory specific gravity of soil using American Society for Testing and Materials.

Attewell, P. B., and Farmer, I. W. 1988. Principles of engineering geology Principles of Engineering Geology. John Wiley & Sons, Inc, New York, 1045pp. ISBN-13: 978-94-009-5709-1 DOl: 101007/978-94-009-5707-7

Bell, F. G. 2007. Engineering Geology Second Edition, Elsevier Limited.

Bell, F. G. 1993. Engineering Treatment of Soils. Spon Press, London.

Bell, F. G. 2004. Engineering Geology and Construction. Spon Press, London.

Brown, S. F. 1996. Soil mechanics in pavement engineering. Geotechnique, 46, 383–426

Carter, M., and Bentley, S. P. 1991. Correlations of soil properties, Pentech Press Publishers,London, 129pp

Chen, D. H., Lin, D. F., Pen-Hwang L. Ph., and Bilyeu, J. 2005. A correlation between Dynamic Cone Penetrometer values and pavement layer moduli. Geotechnical Testing Journal, 38(1).

Daramola, S., Malomo, O., Siyan, A., and Asiwaju-Bello, A. 2015. Engineering Geology of Failed Sections of Isua – Idoani Road Southwestern Nigeria. Journal of Environment and Earth Science, Vol 5, No 19, 9pp. https://doi.org/10.1186/s40703-018-0096-9

De Beer, M., and van der Merwe, C. J. 1991. Use of the Dynamic Cone Penetrometer (DCP) in the design of road structures. Minnesota Department of Transportation, Minnesota.DIN 4094 Part 2, 1980. Dynamic and Static Penetrometer.

Done, S., and Samuel, P. 2006. Department for International Development (DFID), Measuring road pavement strength and designing low volume sealed roads using the dynamic cone penetrometer. Unpublished Project Report, UPR/IE/76/06 Project Record No R7783 wwwtransport-linksorg/ukdcp/docs/Manual/manualhtml

Federal Meteorological Survey, 1982. Atlas of the Federal Republic of Nigeria, 2nd Edition,Federal Surveys, 160pp.

Federal Ministry of Works and Housing, 1997. Nigerian general specifications for roads and Bridges. Federal Highway Department, Lagos, 2: 145-284.

Hassan, A., 1996. The effect of material parameters on dynamic cone penetrometer results for fine-grained soils and granular materials. PhD dissertation, Oklahoma State Univ,Stillwater, Oklahoma.

Ifarajimi, W. T., Oladapo, M. I., and Bayode, S. 2021. Geophysical and Geotechnical Evaluation of Subgrade Integrity Classification of Some Failed Section along Sagamu-Benin Highway Southwestern Nigeria. Minna Journal of Geosciences (MJG) Volume 5 Number 1&2, 75-96pp

Iloeje, P. N. 1981. A new geography of Nigeria. Longman Nigeria Limited, Lagos.

Ilori, A. O. 2015. Geotechnical characterization of a highway route alignment with light weight penetrometer (LRS 10), in southeastern Nigeria. International Journal of Geo-Engineering, 6(7), 28pp http://dxdoiorg/101186/s40703-015-0007-2

Imeokparia, E. G., and Falowo, O. O. 2020. Subsoil Foundation Support Assessment in Owo Area of Ondo State, Southwestern Nigeria. Geotechnical and Geological Engineering, 38(2), pp 2009-2026. https://doi.org/101007/s10706-019-01144-0

Kezdi, A., and Rethati, L. 1988. Handbook of Soil Mechanics, Volume 3: Soil Mechanics of Earthworks, Foundations and Highway Engineering Elsevier, Amsterdam.

Nigerian Geological Survey Agency, 2006. Geological and Mineral Map of Ondo State State,Nigeria

Nigeria Geological Survey, 1984. Geological Map of Southwestern Nigeria, Geological Survey Department, Ministry of Mines, Power and Steel, Nigeria.

Okigbo, N. 2012. Causes of Highway Failures in Nigeria. International Journal of Engineering Science and Technology (IJEST), Vol 4 No 11, pp4695-4703.

Osuolale, O. M., Oseni, A. A., and Sanni, I. A. 2012. Investigation of Highway Pavement Failure along Ibadan - Iseyin Road, Oyo State. Nigeria International Journal of Engineering Research & Technology (IJERT) ISSN: 2278-0181, Vol 1 Issue 8, 1-6pp.

Owoseni, J. O., and Atigro, E. O. 2019. Engineering geological investigation of highway pavement failure in basement complex terrain of southwestern Nigeria. International Journal of Engineering Science and Invention, Volume 8, Issue 6, Series 1, pp 14-22.

Paige-green, P., and Zyl, G. D. V. 2019. A Review of the DCP-DN Pavement Design Method for Low Volume Sealed Roads. Development and Applications. Journal of Transportation Technologies, 9, pp 397-422 https://wwwscirporg/journal/

Putra, J., Ramadhansyah, A. H., and Norhidayah, E. S. 2021. Editorial: Trends and Advanced Materials for Pavement and Road Infrastructure. Frontiers in Materials (8), 1-2.

Transport and Road Research Laboratory, 1990. A user's manual for a program to analyse dynamic cone penetrometer data (Overseas Road Note 8) Crowthorne: Transport Research Laboratory.

Vazirani, V. N., and Chandola, S. P. 2009. Concise Handbook of Civil Engineering. Revised Edition, Rajendra Ravindra Printers Pvt Ltd, New Delhi, India, 1318pp

Williams, L. 1997. Fundamental of Geophysics. Cambridge University Press, 206-217pp.

Wright, P. H. 1986. Highway Engineering. Sixth Edition, John Willey and Sons, New York

Zhdanov, M. S., and Keller, G. V. 1994. The geoelectrical method in geophysics exploration. Elsevier, Amsterdam.

This paper DOI: 10.5281/zenodo.7861995

Journal New Website web1: https://ijgsw.eu.org/

web2: https://ijgsw.net/

Journal Old Website: http://ijgsw.comze.com/ is no longer used

You can submit your paper to email: Jichao@email.com

Or IJGSW@mail.com